Research on the Ensemble Forecasting Method for Green Tide Paths in the Yellow Sea Based on Parameter Perturbation

Yinlin Zhu, Yuheng Wang, Liang Zhao
(College of Marine and Environment, Tianjin University of Science and Technology, Tianjin 300457, China)

Abstract: Yellow Sea green tides have become recurring marine ecological disasters, making accurate forecasting essential for early warning and preventive measures. This study incorporates a stochastic perturbed parameterization scheme into the Yellow Sea Green Tide Drift Model to create an ensemble forecast of the drifting path of green tides, using the 2016 Yellow Sea green tide event as a case study. The ensemble forecast experiment demonstrates that this approach effectively simulates the drift characteristics of the 2016 green tide. Validation with Moderate Resolution Imaging Spectroradiometer (MODIS) remote sensing data reveals that the ensemble forecast significantly enhances the forecasting performance for periods exceeding 15 days, with the average absolute error in the forecast path reduced by 32%.

Keywords: Ecological model; stochastic parameter perturbation method; yellow sea green tide; ensemble forecasting

1 Introduction

Green tides are a new type of ecological disaster caused by the excessive proliferation of large marine green algae. Every year at the turn of spring and summer, the Yellow Sea in China experiences a massive outbreak of green tides, which are caused primarily by *Ulva prolifera*. Currently, the green tides in the Yellow Sea have evolved into normalized marine ecological disasters in the region (Anderson et al., 2002; Pang et al., 2010). The Yellow Sea green tide is a typical transregional marine ecological disaster. Its origin and the location where it becomes a disaster are in different sea areas. Its growth and decay process usually lasts for 2 – 3 months, are involves complex marine processes (Qiao et al., 2009; Liu et al., 2013). Large-scale outbreaks of green tides not only destroy the marine ecosystem around the Yellow Sea but also significantly affect industries, such as maritime events, aquaculture, tourism, and shipping in coastal cities, resulting in serious economic losses (Qiao et al., 2009; Ye et al., 2011; Liu et al., 2013; Paumier et al., 2018; Zhao et al., 2018; Zhan et al., 2024).

In the face of the ecological disaster of green tides in the Yellow Sea, monitoring is currently carried out mainly through onsite observations and satellite remote sensing. Short-term assessments of the extent of green tide outbreaks are subsequently performed on the basis of the green tide images captured onsite and the inverted remote sensing images, followed by preemptive harvesting organized by local governments (Qiao et al., 2009; Liu et al., 2017; Xing et al., 2019; Zhan et al., 2024). However, the arrival time and location of green tides vary greatly each year, and relying solely on monitoring images makes it difficult to judge and predict their drifting paths over the long term (Liu et al., 2015; Xing et al., 2019; Zhan et al., 2024). Therefore, it is extremely necessary to build a forecast model for the drifting path of green tides in the Yellow Sea to predict their drifting direction and changes in advance. Over the years, scholars have attempted to establish various green

tide drift models on the basis of different ocean dynamic models (Lee et al., 2011; Bai et al., 2013; Ji et al., 2018; Zhao et al., 2018; He et al., 2021; Zhou et al., 2021; Gao et al., 2022; Wang et al., 2022; Sheng et al., 2023). These models are mostly based on the Lagrangian method, treating the floating sea mustard on the sea surface as multiple mass points, driven by the wind on the sea surface and the current in the sea surface layer, and performing horizontal physical motion on the sea surface layer. The key parameter values used in the parameterization schemes of the models are mostly obtained from empirical formulas, sensitivity experiments, or observations. By comparing with the actual drift characteristics of the green tide, a better-performing scheme is selected from a multitude of possibilities (Wang et al., 2022; He et al., 2021). However, the sea conditions and weather processes in the Yellow Sea are complex and diverse, leading to large uncertainty in green tide path forecasts using a single deterministic forecast. This forecast uncertainty is amplified as the forecast duration increases, leading to a noticeable decline in forecast performance, with a relatively short time of predictability. At present, green tide path forecasts typically cover only 7 days (Palmer et al., 2014; Wu and Levinson, 2021; Jiao et al., 2022).

Ensemble forecasting is a numerical weather prediction method proposed to reduce forecast uncertainty. It was first introduced by Epstein (1969) and Leith (1974) and is based on stochastic dynamic theory and the Monte Carlo method. By using different models or different initial perturbation techniques, a finite number of forecast samples are constructed, and by creating an "ensemble" of these samples, information is combined and errors are aggregated, transforming a single deterministic forecast into an uncertain forecast (Wu and Levinson, 2021). Studies have shown that ensemble forecasting can not only reduce uncertainty in forecasts and improve the skill of a single deterministic forecast but also extend the duration of useful forecasts. Moreover, it enables the calculation of probabilities for various outcomes on the basis of a range of forecast scenarios, thereby converting a single deterministic prediction into a probabilistic prediction. This approach also allows for a quantitative assessment of the forecast's inherent uncertainty. (Krishnamurti et al., 2000; Weigel et al., 2009; Roiha et al., 2010; Huo et al., 2019; Wu and Levinson, 2021; Liu et al., 2023; Murphy et al., 2024). Currently, ensemble forecasting methods have been widely applied in the fields of typhoon track prediction, subseasonal-to-seasonal forecasting, and marine ecological forecasting. Weber (2003) demonstrated that ensemble forecasting can reduce the 72-hour track forecast error of Atlantic hurricanes by more than 20%. Jacox et al. (2019) discussed the predictability of sea surface temperature (SST) in the California Current region on the basis of the Global Climate Ensemble Forecast System (NMME), establishing a forecasting method on a four-month timescale. Robinson et al. (2021) used a multimodel ensemble approach to predict the potential habitat distribution of the Pacific sand lance (*Ammodytes personatus*) in the Strait of Georgia, British Columbia, Canada, enhancing the accuracy of habitat distribution predictions for the Pacific sand lance. Murphy et al. (2024) developed the Southern Ocean Marine Ecosystem Model Ensemble (SOMEME), aiming to provide a scientific basis for the sustainable management of fishery resources and to ensure the health and biodiversity of the Southern Ocean ecosystem under climate change.

This study uses the Yellow Sea Green Tide Drift Model (YSGTDM) to construct an ensemble forecast of the Yellow Sea green tide drift path, aiming to improve the forecast ability and effective forecast duration of the current Yellow Sea Green tide path forecasts. Through an ensemble forecast experiment of the Yellow Sea green tide drift path combined with green tide remote sensing monitoring data, the improvement effect of the ensemble forecast method on Yellow Sea green tide drift path forecasts is analyzed, and the applicability of this forecast method in the simulation of the Yellow Sea green tide drift path is discussed. The ensemble forecast framework for the green tide path in the Yellow Sea constructed in this paper is a long-term forecast at a scale above the subseasonal-to-seasonal range. To facilitate the comparison and analysis of the performance improvement of different forecast durations using the ensemble forecast approach for green tide path forecasting, the forecast timescale is divided into the following categories on the basis of the division of forecast lead times in meteorology and the characteristics of model simulation results: Forecasts within 5 days after the model begins are defined as short-range forecasts (SRF), forecasts from 5 to 15 days are defined as medium-range forecasts (MRF), forecasts from 15 to 31 days are extended-range forecasts (ERF), forecasts from 32 to 61 days are defined as subseasonal-to-seasonal (S2S) forecasts, and forecasts beyond 61 days are long-range forecasts (LRF). For the prevention and control of green tide disasters, the reference value of path forecasts is more significantly reflected in the initial occurrence and rapid development stages of green tides (from SRF to S2S forecast). In the later stages of green tide outbreaks to the decline phase, government departments organize large-scale efforts to intercept and salvage *U. prolifera* on the sea surface, and the position of the dense area of green tides is greatly influenced by human factors. Therefore, this paper does not present the results and verification of LRFs.

2 Model, data and experimental design

2.1 Yellow Sea Green Tide Drift Model

The YSGTDM uses the Lagrangian particle tracking method, which has a horizontal resolution of 1/36° and a temporal resolution of 1 h. The drift of the Yellow Sea green tide is driven mainly by surface winds and upper ocean currents. At the same time, under the influence of the Coriolis force, the direction of the green tide drift forms an angle with the wind direction. The Lagrangian method is used to calculate the drift path of *U. prolifera* as follows (Wang et al., 2022):

$$\begin{cases} \frac{dx_i}{dt} = R_1 \cdot u_a + R_2 \cdot V_d \cdot \cos(\vartheta_i - \vartheta_0) \\ \frac{dy_i}{dt} = R_1 \cdot v_a + R_2 \cdot V_d \cdot \sin(\vartheta_i - \vartheta_0) \end{cases} \quad (1)$$

where x_i and y_i represent the positions of the *U. prolifera* particle i in the x and y directions at time t, respectively; u_a and v_a represent the current speeds in the x and y directions, with units of m/s; V_d represents the wind speed, with units of m/s; and R_1 and R_2 represent the drag coefficients for the current and wind, respectively, which reflect the deceleration of *U. prolifera* particles during the peak proliferation phase of the green tide, influenced by various factors, such as gravity, wave action, buoyancy, and turbulence; and ϑ_i represents the angle between the wind direction and the x direction. ϑ_0 represents the angle of deflection in the movement direction of

U. prolifera due to the Coriolis effect.

2.2 Model configuration

This study utilizes the Yellow Sea green tide event in 2016 as a case study for ensemble forecast experiments. The simulated area spans 119~125°E, 32~38°N. The model outputs green tide simulation results every hour, encompassing the geographic coordinates and environmental information at the location of each *U. prolifera* particle. For ease of statistical analysis, computation, and comparison with actual conditions, the results provided every day at 00:00 are considered the forecast results for that day, and this approach is not further elaborated upon in subsequent discussions.

The YSGTDM uses input the forcing data for both the current field and the wind field. The current field data are sourced from the high-resolution Regional Ocean Modeling System (ROMS) physical model, which covers an area 105–135°E, 24–41°N, including the Bohai Sea, Yellow Sea, and East China Sea. It has a horizontal resolution of 1/36°, 40 vertical layers, and a temporal resolution of 1 h. After inspection and optimization, this model is capable of effectively reflecting the spatiotemporal distribution and changes in the simulated marine area (Lee et al., 2018; Li et al., 2021). The wind field data are derived from the European Centre for Medium-Range Weather Forecasts (ECMWF) ERA5 single-layer 10 m wind data, with a horizontal resolution of 0.25° and a temporal resolution of 1h.

The initial time, simulation duration and initial release position of *U. prolifera* particles in the model refer to the optimized remote sensing analysis data of green tides (Wang et al., 2022). In 2016, remote sensing first detected the green tide on May 17th (CST), and the last detection of the green tide occurred on July 30th. In the model, these 2 dates are set as the start and end times of the model run, with a total simulation duration of 75 days. To simplify the transport process of green tides in the Yellow Sea within ensemble forecasting experiments, this research currently does not consider variations in the distribution area of green tides. During each model run, a single particle is released to simulate the drift path, thereby concentrating the analysis on the specific changes in the trajectory of green tides. The initial release position of the particle is located at 121.6215°E, 33.5670°N, which is the center of the dense area of the green tide distribution first detected by remote sensing.

2.3 Building ensemble members based on the stochastic parameter perturbation scheme

The uncertainty in the parameter values of the parameterization scheme in the YSGTDM is one of the sources of prediction errors for the drifting path of green tides in the Yellow Sea, and it is a common type of model error. To address model errors caused by the uncertainty of physical process parameterization schemes, the stochastically perturbed parameterization (SPP) scheme is widely used internationally (McCabe et al., 2016). This method builds ensemble members by directly perturbing important parameters in the model through stochastic physical methods while maintaining the internal consistency of the physical parameterization scheme (Buizza et al., 1999; Ollinaho et al., 2016). This perturbation is considered to be a more physically reasonable method from the source of model uncertainty, and many studies have shown that this method can improve the reliability and probabilistic forecasting skills of ensemble forecast systems to a certain extent (Leutbecher et al., 2017; Christensen, 2020; Lang et al., 2021; Peng et al., 2022; Qiao et al., 2023).

According to Equation (1), there are three key parameters in the model: the current drag coefficient, the wind drag coefficient, and the angle of motion deviation caused by the Coriolis force. This study introduces the SPP scheme to perturb these three key parameters to represent the uncertainty in the green tide drifting process.

The ensemble forecast members are typically composed of one control member and multiple ensemble members perturbed from the control member. Calibrating the parameter values and variable values of the control member is the first step in building the ensemble members. On the basis of the relevant literature and previous experiments, the sea current drag coefficient in the green tide drift model usually ranges from 0.8 to 1.0 (Li et al., 2014; Ji et al., 2018; He et al., 2021; Zhou et al., 2021; Wang et al., 2022), and the wind drag coefficient generally ranges from 0.01 to 0.05 (Li et al., 2014; Ji et al., 2018; Zhao et al., 2018). The direction of green tide drift and the wind direction range from 5° ~ 40° (Yi et al., 2010; Liu et al., 2023). The parameter values of the ensemble control member β_{ctr}, the standard deviation of the parameter perturbation σ, and the range of the parameter perturbation are determined by sensitivity experiments, as shown in Table 1.

Table. 1 Parameters chosen within the SPP framework.

Parameter/ variable	Physical description	β_{ctr} (μ)	σ	[min, max]
R_1	current drag coefficient	0.4	0.1	[0.3, 0.55]
R_2	wind drag coefficient	0.02	0.01	[0.005, 0.03]
ϑ_0	deflection angle caused by wind action	25°	15°	[5°, 45°]

After the parameter values of the ensemble control member β_{ctr}, the perturbation standard deviation σ, and the range of perturbations are determined, the SPP scheme is further introduced to construct the ensemble members. In the model, each parameter is independently perturbed without interference, which is different from the random perturbation field that changes with time or space in the atmospheric model (Ollinaho et al., 2016; Peng et al., 2022). In this study, the parameter values do not change with time or space after the initial setting. The specific method is as follows. First, 50 normally distributed random numbers φ_k (k=1, 2, …, 50) with a mean of β_{ctr} and a standard deviation of σ are generated, and those that fall outside the [min, max] constraint interval are discarded (Peng et al., 2022). The remaining random numbers are the random perturbation values β_k for that parameter. The perturbed parameter values are then randomly combined, and the parameterization scheme constructed by the combination is the parameterization scheme for each ensemble member. The formula is as follows:

$$\beta_k = \varphi_k \qquad \varphi_k \sim N(\mu, \sigma^2), \beta_k \in [\min, \max] \tag{2}$$

where β_k is the random perturbation value, with a numerical range between the minimum and maximum perturbation values; φ_k is the perturbation random number, which conforms to a normal distribution; μ is the perturbation mean; and σ is the perturbation standard deviation. Considering the maximization of the ensemble members' dispersion and the computational cost (Milliff et al., 2011), the Yellow Sea green tide drift path ensemble forecast experiment consists of 15 ensemble members, including 1 control member and 14 perturbation members.

2.4 Experimental design and verification

This research encompasses a comprehensive experimental framework consisting of 15 distinct

trials. The first set is the control experiment, which provides the green tide path forecast results from the ensemble control member selected by the sensitivity experiment without any perturbation. The 2nd to 15th sets are the ensemble experiments that introduce the SPP scheme and simultaneously perturb 3 key parameters to obtain the green tide path forecast results of the 14 perturbation members. Each simulation is conducted once, and none of the 15 experiments use initial value perturbations, as shown in Table 2.

Table. 2 Design of the Yellow Sea Green Tide Drift Path Experiment

Test type	Test group	Model physical disturbance scheme	Initial disturbance
CTL	1	None	None
SPP	2~15	Disturbance of key parameters	None

The verification method used in this study evaluates the forecast effectiveness of both single model forecasting methods and ensemble forecasting methods by calculating the errors between the forecasted and actual positions. The error calculation includes the absolute error in distance and the distance errors in both the meridional and zonal directions. Owing to the significant influence of weather conditions on the satellite remote sensing monitoring of green tides, it is difficult to obtain continuous observational data. Therefore, this paper uses only the green tide remote sensing observation data from days that are less affected by weather conditions, which represent the drifting characteristics of the green tide during different periods. The actual drifting path of the green tide is determined by the center position of the dense area of the green tide calculated for the day, and the simulation outcomes of the model are verified on this basis.

The satellite remote sensing data used in the study come from Moderate Resolution Imaging Spectroradiometer (MODIS) sensor data (https://ladsweb.modaps.eosdis.nasa.gov/search/), which are freely available from the National Aeronautics and Space Administration (NASA) (Hu et al., 2010). MODIS is a sensor onboard the Terra and Aqua satellites and features 36 bands, all at moderate resolution. The Terra and Aqua satellites alternate in their overpasses, with a frequency of twice a day. The selected remote sensing image inversion data are the MODIS Level 1B HDF data from the Terra and Aqua satellites under cloud-free or cloudy conditions, with a spatial resolution of 250 m. It includes data from MODIS bands 1 and 2, with spectral ranges of 620–670 nm and 841–876 nm, respectively, corresponding to the red and near-infrared bands. After geometric correction of the MODIS data images, the normalized difference vegetation index (NDVI) is employed to extract the green tide information in the Yellow Sea (Xing and Hu, 2016).

3 Forecast results

3.1 Deterministic forecast results of the Yellow Sea green tide path

Fig. 1 compares the drifting paths of the green tide given by the two forecasting methods with the actual path. Fig. 1a shows the single deterministic green tide path forecast given by a single model, which is also the control member forecast result of the ensemble, referred to as the control forecast in the following text, and Fig. 1b shows the ensemble mean forecast of the green tide, which is obtained by directly calculating the arithmetic mean of all ensemble members. Fig. 1 shows that the control forecast given by the YSGTDM and the ensemble mean forecast of the Yellow Sea green

tide reflect the drifting characteristics of the green tide in 2016 quite well. After the model releases the *U. prolifera* particles at the initial position, the particles continue to drift northward with the sea surface current. During the northward movement, the particles tend to move first westward and then eastward, with the turning position located at approximately 35° N and the landing location in the sea area of Weihai city, Shandong Peninsula.

The remote sensing positions of the green tide are compared with the forecast positions in Fig. 1a and Fig. 1b. The main differences between the control forecast and the ensemble forecast lie in the drifting trajectory and the movement speed of the green tide. With respect to the drifting trajectory of the green tide, the ensemble average path does not significantly differ from the control forecast path overall, but both the ensemble average path and the point of landfall of the green tide are further east than the control forecast. As the forecast duration increases, the particle speed in the control forecast is noticeably faster than that in the ensemble forecast. The control forecast predicts that the dense area of the green tide will reach the shore within the S2S, whereas the ensemble average path shows that the dense area of the green tide remains offshore of Weihai city without making landfall by the end of the simulation.

We further analyze the changes in the simulated positions across various forecast periods. There is little difference between the drift trajectories of the two prediction methods in terms of the SRF and MRF. The simulated positions are located south of the remote sensing position, indicating that the drift speed of the simulated particles in both the control forecast and the ensemble forecast is slower than the actual speed in these two periods.

In the ERF, the simulated positions of both the control member and the ensemble average are to the west of the actual position. In terms of the direction of particle movement, the ensemble average position is comparable to the remote sensing position on June 17, whereas the control forecast position is north of the remote sensing position. This indicates that there is a significant difference in the simulated particle speed between the control forecast and the ensemble forecast during this period, with the ensemble forecast providing a better simulation of the green tide position than the control forecast does.

In the S2S forecast, there are differences between the ensemble forecast and the remote sensing position of the green tide, but the distance between the two is always relatively small. In contrast, the position predicted by the control forecast is quite far from the actual position. On the basis of the movement trajectory of the simulated particles, the ensemble forecast position does not exceed 36°N by June 25, whereas the control forecast position is already near the actual position by July 2. On July 2, the positions of the control forecast and the ensemble forecast are northeast and southeast of the actual position, respectively, indicating that during this forecast period, the control forecast simulates a significantly faster northward drift speed of the green tide than the ensemble forecast does.

In summary, both the single deterministic forecast and the ensemble mean forecast can simulate the drifting characteristics of the green tide in 2016 quite well. The ensemble forecast method simulates the drifting trajectory of the green tide more closely to the actual situation, and the forecast

quality of the green tide path is higher than that of the prediction using a single model. The ensemble forecast method mainly improves the path forecast after the ERF period, but the improvement effect is not obvious for at the SRF and MRF scales.

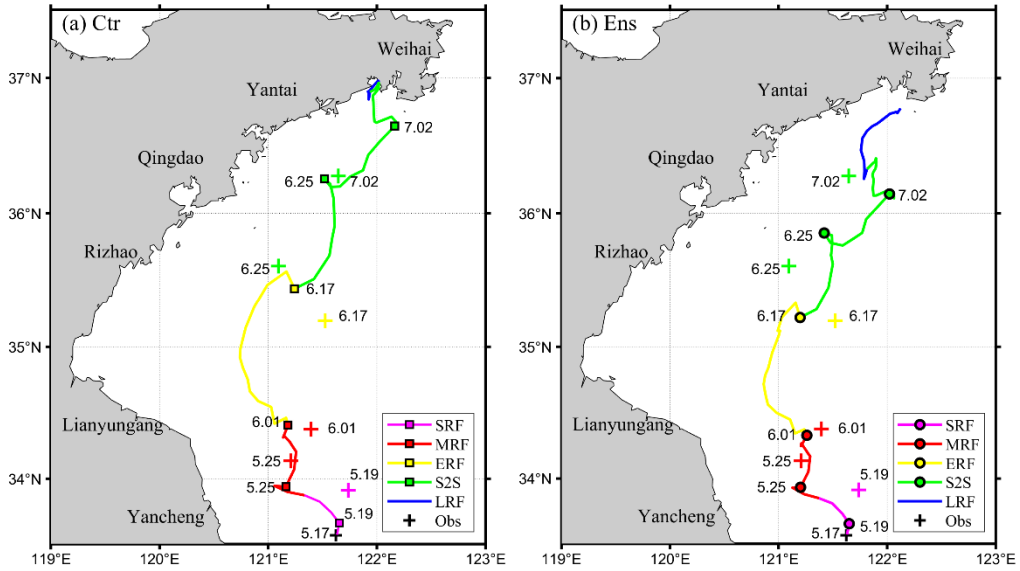

Fig. 1. Compares the control forecast path (a) and the ensemble mean forecast path (b) with the satellite remote sensing positions of the green tide. The same colored segments and symbols represent the same forecast lead time, and the positions marked on the solid line correspond to the remote sensing positions of the same day, with the remote sensing positions marked as "+". In the legend, SRF, MRF, ERF, S2S, and LRF represent different forecast durations, which are short-range forecasts, medium-range forecasts, extended-range forecasts, subseasonal-to-seasonal forecasts, and long-range forecasts, respectively.

3.2 Probabilistic forecast results of the Yellow Sea green tide path

Using mathematical statistical methods, it is possible to calculate a probabilistic forecast of the Yellow Sea green tide path. First, the Yellow Sea area needs to be gridded, and the horizontal resolution of each grid is defined as 1.75°. The probability of the occurrence of dense green tide areas is defined as the ratio of the number of ensemble members within the grid to the total number of ensemble members. The more ensemble members that appear within the grid, the greater the probability that dense green tide areas have passed through that grid. Fig.2 shows the probability forecast of the potential path of the green tide dense area, with a forecast period from May 18 to July 30. This study classifies the probability of the green tide dense area passing through a point into 5 forecast levels: very high probability (>50%), high probability (37.5%~50%), moderate probability (25%~37.5%), and low probability (<25%), and no color indicates that there is no green tide dense area passing through that grid.

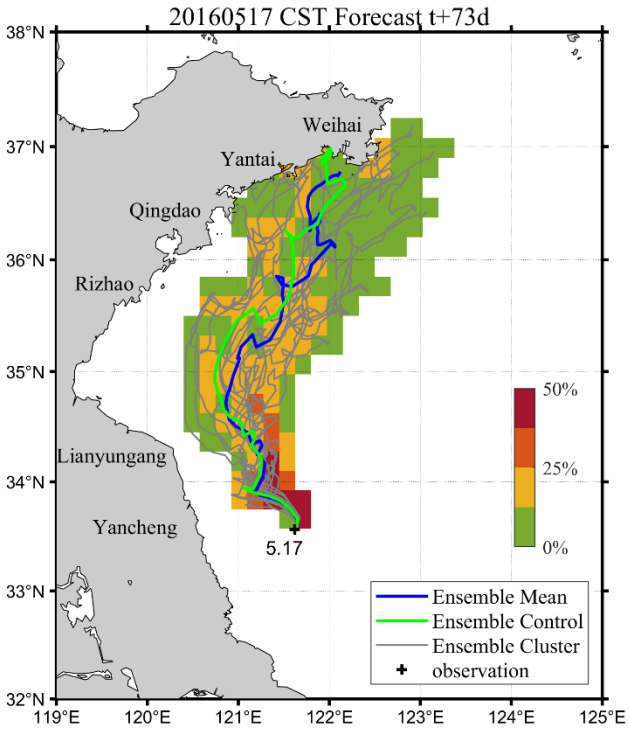

Fig. 2. Probabilistic forecast of the path of the green tide dense area. The valid forecast duration is May 17, 2016 + 73 d. The blue solid line represents the ensemble mean forecast path, which is obtained by calculating the average of all ensemble member forecast paths. The green solid line represents the control forecast path provided by the control member. The gray solid lines represent the individual forecast paths given by each ensemble member. The center position of the green tide distribution observed by remote sensing on May 17 is marked with the "+". The color bar delineates the probability forecast levels for the passage of dense green tide areas: red indicates a very high probability (>50%), orange signifies a high probability (37.5%~50%), yellow represents a moderate probability (25%~37.5%), green denotes a low probability (< 25%), and the absence of color implies that no dense green tide areas will pass through.

The drifting paths of the green tide over the entire 75-day forecast for the 14 ensemble member forecasts, control forecast, and ensemble mean forecast are depicted in Fig. 2. The *U. prolifera* particles in the control member and the 14 ensemble members are released at the same location on May 17. In the initial phase of the simulation, all the members exhibit a high degree of similarity, with the forecasted green tide paths generally drifting northward. The paths initially veer westward to approximately 35° N before turning eastward, which is consistent with the previous description. The distribution of the green tide trajectories simulated by the 15 members clearly reveals that as the forecast duration increases, the drifting paths of the green tide begin to diverge. The path forecast uncertainty is amplified with the extension of the forecast time. The ensemble forecasting method scientifically describes the uncertainty of the green tide patches during the actual drifting process.

According to the calculated probabilistic forecast results of the drifting paths, the dense green

tide area in 2016 mainly approaches the Shandong Peninsula from the central Yellow Sea, with the dense green tide area reaching the coast in the region of Qingdao city to Weihai city. The probabilistic forecast can accurately predict the sea areas through which the dense green tide area will drift, providing a scientific basis for early interception and the organization of salvage work related to green tide prevention and control. Additionally, the probabilistic forecast quantitatively calculates the magnitude of uncertainty in the green tide path forecast, which is an important improvement over the single deterministic forecast of green tide drifting.

3.3 Yellow Sea green tide path forecast error

The error between the forecast path and the actual position is a critical reflection of the predictive ability of the model regarding the drifting path of green tides. Fig. 3 shows the cumulative absolute error between the 14 ensemble members, the control forecast, and the ensemble mean forecast with actual conditions over different forecast periods. It comprehensively demonstrates the magnitude of the absolute error between the ensemble forecast members and actual conditions at various forecast times, as well as the overall simulation effect. According to Fig. 3, it is evident that the absolute error for the 14 ensemble members and the control member in the SRF period are quite similar, averaging 30.2 km. The MRF period has the smallest absolute error among all forecast periods, where the absolute error of the 9th member from the actual situation on June 1 is merely 5.0 km. After the ERF period, the absolute error between the ensemble member forecasts and the actual situation gradually increases, with the 1st and 6th members having the largest error distances in the ERF and S2S periods, respectively. The cumulative absolute error of the ensemble average over 5 forecast periods is 194.4 km, which is lower than those of all the ensemble members and the control member. Moreover, the absolute errors tested over the 6 periods are similar in magnitude, averaging 32.4 km without any extreme cases, which is 16.4 km less than the average absolute error of the control forecast. Compared with the ensemble average, the cumulative absolute error of the 8th member is 195.6 km, which is smaller than that of all the ensemble members and the control member but slightly larger than that of the ensemble mean forecast. Additionally, the absolute errors of these member distribution characteristics are most similar to the ensemble average, with a relatively uniform error distribution across different forecast periods. Therefore, the 8th ensemble member performs the best among the 15 ensemble forecast members.

To analyze the applicability of the two forecasting methods, a daily analysis was conducted on 6 days in Fig. 3, to compare the differences between the ensemble mean forecast and the single deterministic forecast. Although the accumulated absolute error of the ensemble average forecast is less than that of the control forecast, the absolute error in the distance between the ensemble forecast and the actual situation is not always less than that of the control forecast at different forecast durations. As shown in Fig. 4, the absolute error of the ensemble forecast is slightly greater than the control forecast error in the SRF and MRF periods. After the ERF period, the absolute error in the distance for the ensemble forecast is significantly less than that of the control forecast. On June 25, the absolute error of the ensemble forecast decreases by 47.1% compared with that of the control forecast. Overall, the absolute error distance of both the ensemble and control forecasts first

decreases and then increases with the forecast time, and the time when the minimum absolute error occurs for the two forecasting methods is not synchronized; the minimum absolute error of the ensemble forecast occurs during the extension period, lagging behind the control forecast.

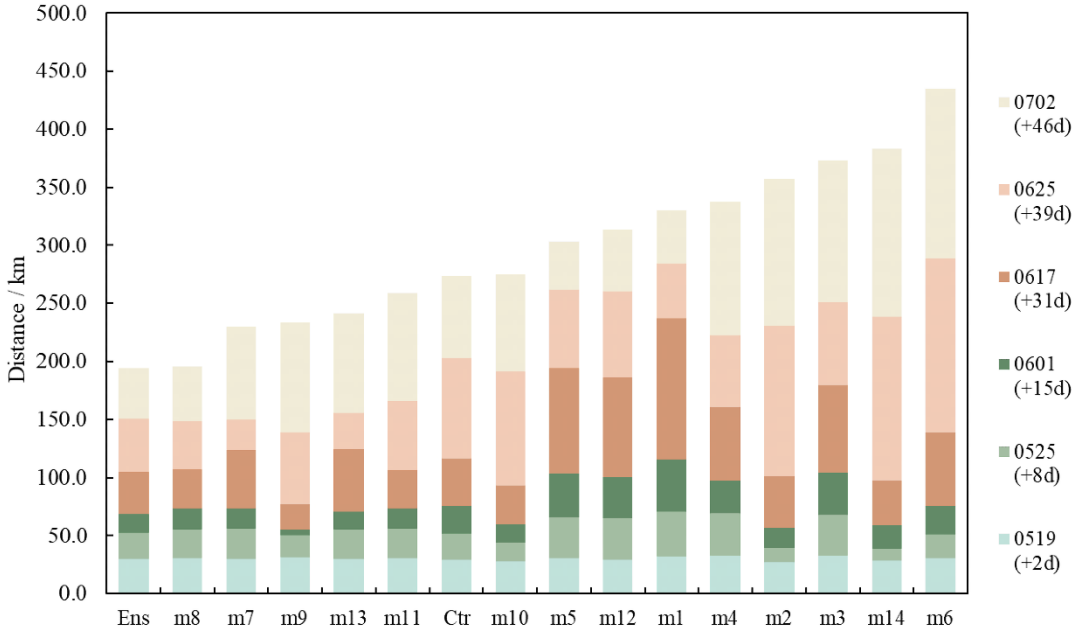

Fig. 3. Cumulative absolute error of 14 ensemble members, control member, and ensemble mean.

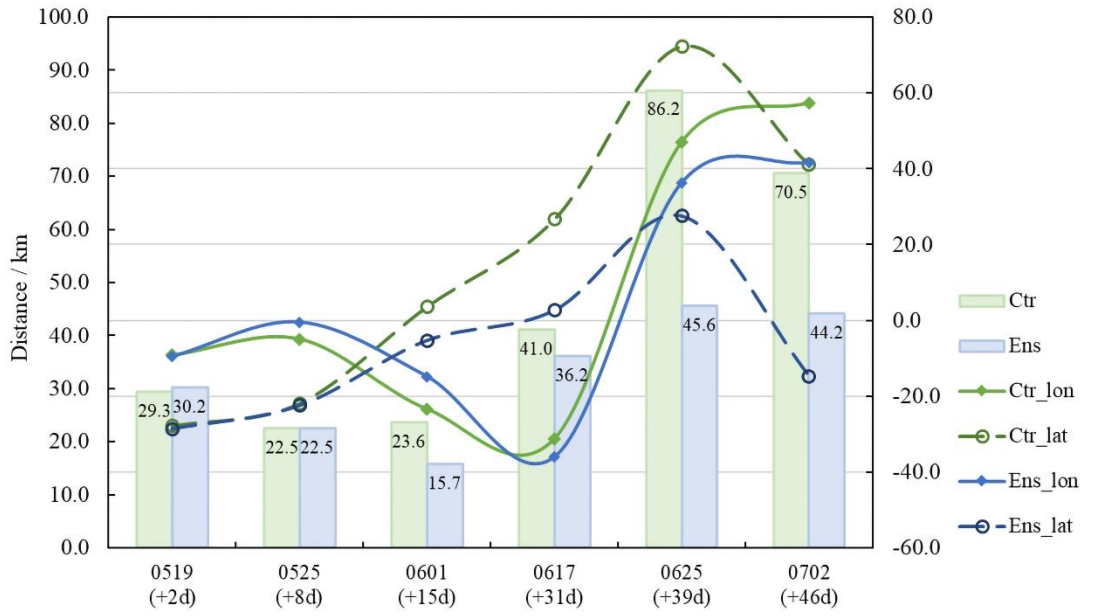

Fig. 4. Absolute error of control forecast and ensemble forecast (bar chart, left axis), as well as meridional and zonal errors (line chart, right axis).

To explore the reasons for the characteristics of the changes in the absolute error in the distance, Fig. 4 simultaneously displays the error in the east–west and north–south directions. Here, a positive error indicates that the forecasted position is east or north of the actual position, whereas a negative error indicates the opposite direction. The slope of the error curve represents the change in the speed of the simulated green tide drift. Fig. 4 shows that the velocity directions in the east–west and north–

south directions are relatively consistent between the control forecast and the ensemble forecast, but there are differences in the magnitude of the speed. The average error in the east–west distance between the two forecasting methods is 7.4 km, which is not a significant difference. In the early stages of the forecast, the forecasted positions of both methods are west of the actual situation, and in the ERF period, the position between the simulation and the actual situation shifts from west to east, with the control forecast turning earlier than the ensemble forecast. In terms of the north–south error, the changes in the SRF period of the ensemble and control forecasts are almost the same. However, from May 25 to June 25, the north–south error changes in the control forecast are significantly faster than those in the ensemble forecast, with a steeper slope in the error, indicating that the control forecast simulates a faster northward drifting speed of the green tide than the ensemble forecast does.

According to the error test results, the ensemble forecasting method based on the SPP scheme does not significantly improve the forecasting ability in the SRF or MRF periods. However, it significantly improves the forecast effect for predictions beyond 15 days, with the absolute error being within 50 km and superior that of to the single deterministic forecasting method. The ensemble forecast mainly improves the path forecast of the green tide drift by reducing the simulated speed of the green tide drifting northward.

4 Discussion

4.1 Ensemble spread

Within a reasonable range of parameter perturbations, ensemble forecasting generally does not exhibit excessive divergence among ensemble members. The spread, which is calculated for different forecast periods, can be used to measure the uncertainty of variables in the forecast. The ensemble spread is the standard deviation of the various variables in the model output, representing the degree of divergence of the ensemble samples, and is an important indicator for increasing confidence in the ensemble mean forecast. The larger the spread is, the lower the predictability. The formula is as follows,

$$spread = \sqrt{\frac{1}{N-1}\sum_{i=1}^{N}(\hat{y}_i - \bar{y}_i)^2} \quad (3)$$

here, N is the total number of ensemble members, $\hat{y}_i$ is the forecast value of the i-th ensemble member, and $\bar{y}_i$ is the ensemble average of the forecast values of the ensemble members. In this study, the dispersion of the ensemble forecast for the green tide drift path is represented by calculating the distance between the forecasted position of each ensemble member and the ensemble average forecasted position.

In Fig. 5a, the path distribution characteristics of all the ensemble members across different forecast periods are illustrated. Correspondingly, Fig. 5b presents the spread of the ensemble members' forecasted paths for each period. Overall, the initial spread of *U. prolifera* particles is relatively small due to the limited release positions. However, the ensemble spread increases rapidly once the model is initiated. During the SRF and MRF periods, the simulated green tide paths of the 15 ensemble members are relatively concentrated, with a small spread, averaging only 4.4 km and

16.1 km, respectively. By the ERF period, the simulated paths of the 15 members show significant divergence. The *U. prolifera* particles from the different models drift northward at noticeably different speeds, and the spread in Fig. 5b for this period increases rapidly from 21.0 km to 49.1 km. The spread among the ensemble members subsequently continues to increase and reaches its maximum value of 80.4 km on day 46 during the S2S period. Later, during the LRF period, as the *U. prolifera* particles gradually reach the southern sea area of the Shandong Peninsula, the ensemble spread briefly decreases before rising again.

The reason for the change in the ensemble spread during the LRF period is due to the physical boundary constraints. In reality, *U. prolifera* cannot cross these boundaries. *U. prolifera* particles, after reaching the shore (and being blocked by the physical boundary), return to the sea to continue moving with ocean currents. As shown in Fig. 5a, some ensemble members simulate the drift of the green tide and have already landed on the coastal areas of the Shandong Peninsula during the S2S period. The coastal current speed is not as fast as that in the open sea, so the position change of these particles is relatively small. On the other hand, other model particles that have not reached the shore continue to drift toward the Shandong Peninsula with the sea surface flow field. The east–west distance does not change significantly, whereas the north–south distance gradually decreases, resulting in an overall trend of decreasing spread. By the 67th day, most of the members have arrived at the Shandong Peninsula, but a few members do not land on the Shandong Peninsula and continue to drift northeastward at sea, so the overall spread increases again.

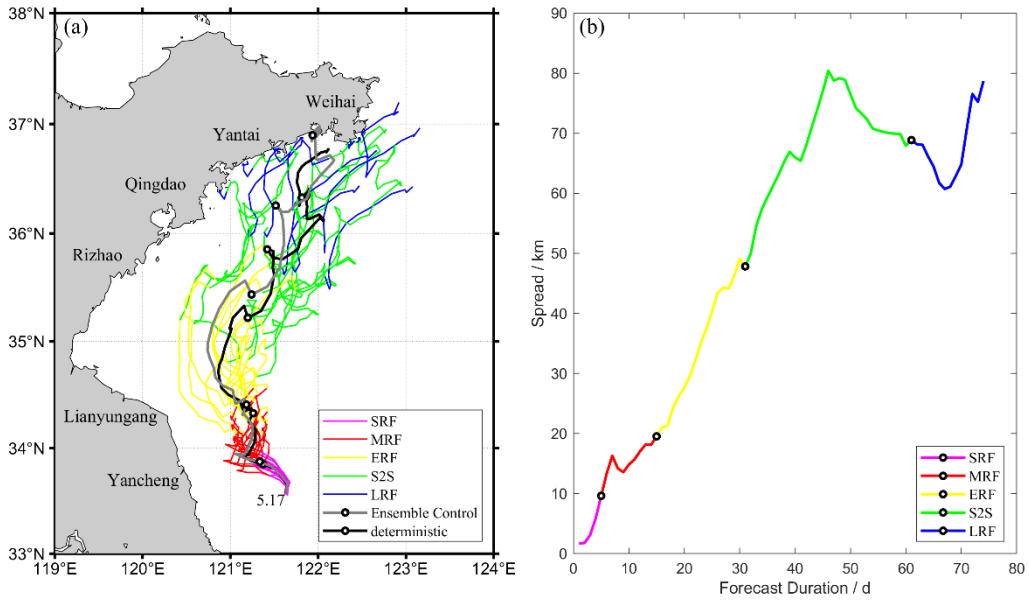

Fig. 5. (a) The green tide forecast paths for ensemble members, control member, and ensemble mean across different forecast periods; (b) The ensemble dispersion of the Yellow Sea green tide path ensemble forecast model across different forecast periods.

4.2 Number of ensemble members

In terms of statistical averages, ensemble forecasts need to construct a sufficient number of ensemble members within a reasonable range to reflect all situations that have actual possibilities. However, in practical applications, the number of ensemble members needs to be reasonable on the basis of the different forecast targets and the limitations of computation, operation, and maintenance costs. In general, a minimum of 10 ensemble members is required to more effectively quantify the spread in ensemble forecasting (Milliff et al., 2011). This paper constructs an effective number of members of 15, to reduce computational costs and shorten the running time of ensemble forecasts, further explores how many members need to be selected for integration to achieve a stable and better forecast effect, and compares the path error situations of forecast results integrated using 1 to 15 members (Qi et al., 2014; Zhang and Yu, 2017).

In this work, the ensemble forecast method is selected to improve the forecast period with significant effects, and path error statistics are obtained accordingly, as shown in Fig. 6. In the statistics, 1 member is used as the control member in the ensemble forecast, whereas members 2 to 14 are the average error values of all random combinations among the 15 ensemble forecast members. For example, when conducting an ensemble with 14 members, the existing 15 ensemble members can be randomly combined to generate 14 distinct results of the ensemble mean path. The absolute error between each of these 14 results of the ensemble mean path and the observed path is subsequently calculated individually. Ultimately, the average of these 14 absolute errors is computed, yielding the path error statistic for the ensemble comprising 14 members. The calculation method for the path error with other numbers of ensemble members follows the same logic.

According to the statistical results, the absolute error between the ensemble forecast simulated green tide positions and the actual conditions exhibits similar variation characteristics at the 4 different times. As the number of ensemble members increases, the absolute error in the forecast path initially significantly fluctuates. However, once a certain threshold of members is reached, the absolute error begins to stabilize. Fig. 6 shows that when 1~7 members are used for the ensemble, the forecast error for the green tide path in the Yellow Sea is highly unstable and subject to large variations. Beyond 7 members, the magnitude of these fluctuations diminishes progressively. When the ensemble size reaches 10~15 members, the path error achieves a stable state. Therefore, the ensemble forecast of the green tide path in the Yellow Sea using 12 ensemble members is nearly saturated, and further increasing the number of members does not significantly improve the forecast effect of the green tide path. This finding further clarifies that in the ensemble forecast of the Yellow Sea green tide path, which is based on the SPP scheme, reducing the error of the green tide drift path by merely increasing the number of ensemble members is limited.

In summary, ensemble forecasts of the green tide drifting path in the Yellow Sea requires at least 10 members to ensure that the ensemble forecast can stably control the forecast error. On the basis of this statistic, provided that the discretization of the perturbation parameter values is appropriate, follow-up studies can control the number of ensemble members within the range of 10 to 13 members according to actual forecast application needs, which can improve the operational efficiency of path forecasting and reduce the computational and maintenance costs of forecasts.

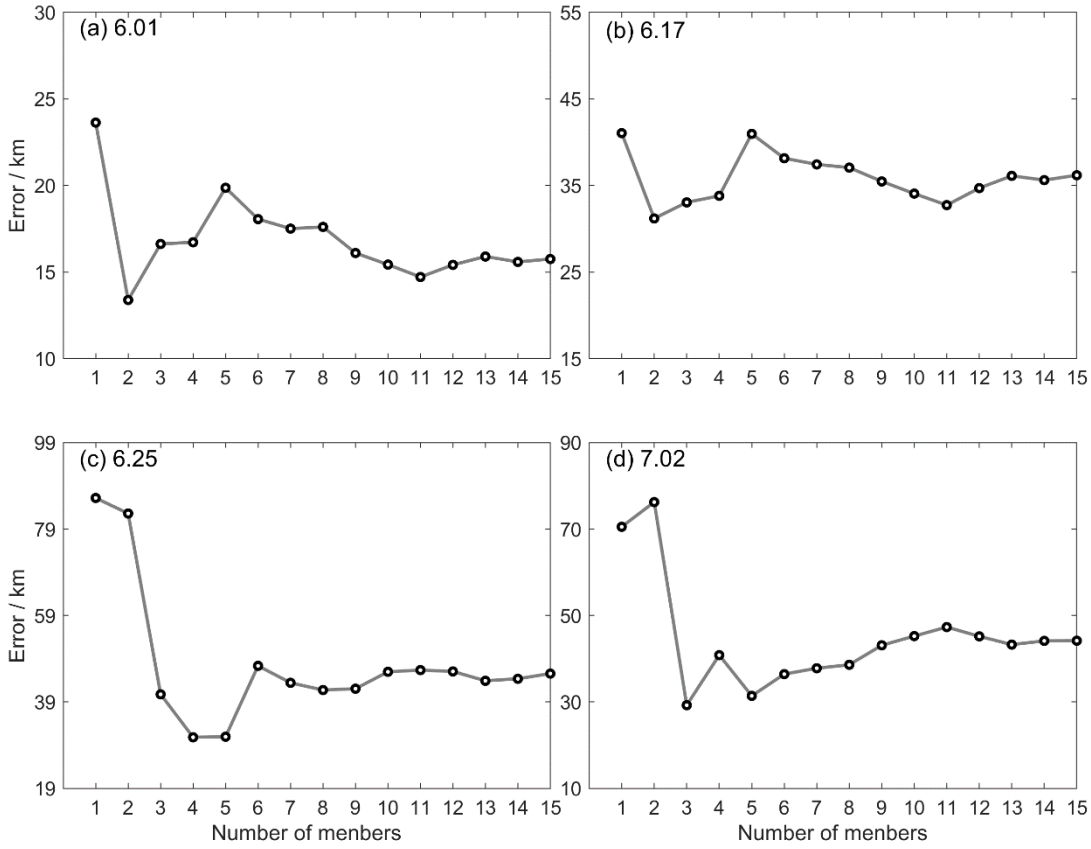

Fig. 6. The impact of the number of ensemble members on the error of the green tide drift path comparison.

5 Conclusion

This study introduces a stochastic perturbation parameter scheme for key parameters in the YSGTDM, constructing an ensemble forecast of the Yellow Sea green tide drift path. The results show that the ensemble forecast of the Yellow Sea green tide drift path provides ensemble mean and probabilistic forecasts that can better simulate the drift characteristics of the Yellow Sea green tide in 2016, showing high consistency with actual observations. The probabilistic forecast of the drift path in dense green tide areas is a significant advantage over single deterministic forecasts, as it quantitatively forecasts the uncertainty in the green tide drift process and provides more scientific guidance for the prevention and mitigation of green tide related ecological disasters.

Using MODIS remote sensing data, a comparative verification was conducted between the single model method and the ensemble forecast method. The ensemble forecast method effectively enhanced the forecast skill for forecast periods of more than 15 days, extending the effective forecast duration of existing path forecasts. Compared with the use of a single model, ensemble forecasting improved the northward drift speed of the green tide, and the forecast error of the green tide drift path for forecast periods over 15 days was reduced by an average of 32%.

In this study, we initially applied ensemble forecasting methods to simulate the drift path of the green tide in the Yellow Sea, revealing significant advancements in the existing forecasting techniques for this phenomenon. However, the long-term transport of Yellow Sea green tides on the

sea surface is a complex process. It involves not only the dynamic influences of sea surface currents and winds on the drift of green tides but also the ecological responses of *U. prolifera* to the marine environment. As the Yellow Sea green tide grows and decays, it alters the overall distribution and movement speed of the green tide, thereby affecting its overall drift trajectory. This aspect was not considered in the current study, where the simulation of single particles was used to simplify the experimental design.

In future research, building upon existing ensemble forecasting methods for the Yellow Sea green tide drift path, we will further explore the integration of ecological processes. This integration aims to broaden the application of Yellow Sea green tide forecasting in operational settings and provide a robust scientific foundation for the prevention and management of ecological disasters associated with Yellow Sea green tides.

Acknowledgements

This work is supported by National Key Research and Development Program of China (2023YFC3108203), and the financially supported by Laoshan Laboratory (LSKJ202202104).

CRediT authorship contribution statement

Yinlin Zhu: Writing – review & editing, Writing – original draft, Visualization, Validation. **Yuheng Wang:** Writing – review & editing, Validation, Software, Methodology. **Liang Zhao:** Writing – review & editing, Supervision, Funding acquisition, Data curation, Conceptualization.

References

Anderson, D. M. et al. (2002). Harmful algal blooms and eutrophication: Nutrient sources, composition, and consequences. *Estuaries, 25*(4), 704-726. doi:10.1007/BF02804901

Bai, T. et al. (2013). Operational Forecast System for green tides in the Yellow Sea. *Marine Forecasts, 30*, 51-58. doi:10.11737/j.issn.1003-0239.2013.01.007

Buizza, R. et al. (1999). Stochastic representation of model uncertainties in the ECMWF ensemble prediction system. *Quarterly Journal of the Royal Meteorological Society, 125*(560), 2887-2908. doi:https://doi.org/10.1002/qj.49712556006

Christensen, H. M. (2020). Constraining stochastic parametrisation schemes using high-resolution simulations. *Quarterly Journal of the Royal Meteorological Society, 146*(727), 938-962. doi:https://doi.org/10.1002/qj.3717

Epstein, E. S. (1969). Stochastic dynamic prediction1. *Tellus, 21*(6), 739-759. doi:10.3402/tellusa.v21i6.10143

Gao, S. et al. (2022). Risk Dynamic Evaluation of Enteromorpha Prolifera Disaster Based on 'Growth-Drift' Prediction Model. *Journal of Ocean Technology, 41*(03), 75-82. doi：10.3969/j.issn.1003-2029.2022.03.009

He, E. et al., 2021. Numerical simulation and forecasting of drift, growth, and death of Enteromorpha in the Yellow sea. *Oceanologia Et Limnologia Sinica, 52*(1), 39–50. doi: 10.11693/hyhz20200300090

Hu, C. et al. (2010). On the recurrent *Ulva prolifera* blooms in the Yellow Sea and East China Sea.

Journal of Geophysical Research: Oceans, 115(C5). doi:https://doi.org/10.1029/2009JC005561

Huo, Z. et al. (2019). Ensemble Forecasts of Tropical Cyclone Track with Orthogonal Conditional Nonlinear Optimal Perturbations. *Advances in Atmospheric Sciences, 36*(2), 231-247. doi:10.1007/s00376-018-8001-1

Jacox, M. G. et al. (2019). On the skill of seasonal sea surface temperature forecasts in the California Current System and its connection to ENSO variability. *Climate Dynamics, 53*(12), 7519-7533. doi:10.1007/s00382-017-3608-y

Jiao, Y., et al., 2022. Influencing factors and prediction method of the green tide scale in the Yellow Sea. Marine Sciences. 46(5), 65–73. https://doi.org/10.11759 / hykx20210718001.

Ji, H. et al. (2018). Numerical simulation of the green tide drift and diffusion in the sea areas of Jiangsu Province. *Marine Sciences, 42*, 82-91. doi: 10.11759/hykx20171118001

Krishnamurti, T. N. et al. (2000). Multimodel Ensemble Forecasts for Weather and Seasonal Climate. *Journal of Climate, 13*(23), 4196-4216. doi:https://doi.org/10.1175/1520-0442(2000)013<4196:MEFFWA>2.0.CO;2

Lang, S. T. K. et al. (2021). Revision of the Stochastically Perturbed Parametrisations model uncertainty scheme in the Integrated Forecasting System. *Quarterly Journal of the Royal Meteorological Society, 147*(735), 1364-1381. doi:https://doi.org/10.1002/qj.3978

Lee, J.H. et al. (2018). 4DVAR Data Assimilation with the Regional Ocean Modeling System (ROMS): Impact on the Water Mass Distributions in the Yellow Sea. *Ocean Science Journal, 53*(2), 165-178. doi:10.1007/s12601-018-0013-3

Lee, J. et al. (2011). On physical factors that controlled the massive green tide occurrence along the southern coast of the Shandong Peninsula in 2008: A numerical study using a particle-tracking experiment. Journal of Geophysical Research (Oceans), 116, 12036. doi:10.1029/2011JC007512

Leith, C. E. (1974). Theoretical Skill of Monte Carlo Forecasts. *Monthly Weather Review, 102*(6), 409-418. doi:https://doi.org/10.1175/1520-0493(1974)102<0409:TSOMCF>2.0.CO;2

Leutbecher, M. et al. (2017). Stochastic representations of model uncertainties at ECMWF: state of the art and future vision: Stochastic Representations of Model Uncertainties. *Quarterly Journal of the Royal Meteorological Society, 143*. doi:10.1002/qj.3094

Li, A. et al. (2021). Recent improvements to the physical model of the Bohai Sea, the Yellow Sea and the East China Sea Operational Oceanography Forecasting System. *Acta Oceanologica Sinica*, 40(11), 87-103. doi:10.1007/s13131-021-1840-0

Li, Y. et al. (2014). Effect of wind on the drifting of green macroalgae in the Yellow Sea. *Marine Environmental Science, 33*(05), 772-776. doi:10.13634/j.cnki.mes.2014.05.022

Liu, D. et al. (2013). The world's largest macroalgal bloom in the Yellow Sea, China: Formation and implications. *Estuarine, Coastal and Shelf Science, 129*, 2-10. doi:https://doi.org/10.1016/j.ecss.2013.05.021

Liu, H. et al. (2023). High-resolution remote sensing of the transportation of floating macroalgae: Case studies with the Ulva prolifera green tide. *National Remote Sensing Bulletin, 27*(01), 187-196. doi: 10.11834/jrs.20235001

Liu, J. et al. (2023). A Recombination Clustering Technique for Forecasting of Tropical Cyclone Tracks Based on the CMA-TRAMS Ensemble Prediction System. *Journal of Meteorological Research, 37*(6), 812-828. doi:10.1007/s13351-023-3064-z

Liu, X. et al. (2015). Cruise observation of Ulva prolifera bloom in the southern Yellow Sea, China. *Estuarine, Coastal and Shelf Science, 163*, 17-22. doi:https://doi.org/10.1016/j.ecss.2014.09.014

Liu, X. et al. (2017). The distribution of green algal micro-propagules and macroalgae at the early stage of green tide in the coastal area of South Jiangsu Province in 2014. *Journal of Ocean University of China, 16*(1), 81-86. doi:10.1007/s11802-017-3008-2

McCabe, A. et al. (2016). Representing model uncertainty in the Met Office convection-permitting ensemble prediction system and its impact on fog forecasting. *Quarterly Journal of the Royal Meteorological Society, 142*(700), 2897-2910. doi:https://doi.org/10.1002/qj.2876

Milliff, R. F. et al. (2011). Ocean ensemble forecasting. Part I: Ensemble Mediterranean winds from a Bayesian hierarchical model. *Quarterly Journal of the Royal Meteorological Society*, 137(657), 858-878. doi:https://doi.org/10.1002/qj.767

Murphy, K. et al. (2024). Developing a Southern Ocean Marine Ecosystem Model Ensemble To Assess Climate Risks and Uncertainties. *ESS Open Archive,* May 15. doi: 10.22541/essoar.171580194.49771608/v1

Ollinaho, P. et al. (2016). Towards process-level representation of model uncertainties: Stochastically perturbed parametrisations in the ECMWF ensemble: Process-level representation of model uncertainties. *Quarterly Journal of the Royal Meteorological Society,* 143. doi:10.1002/qj.2931

Palmer, T. N. et al. (2014). The real butterfly effect. *Nonlinearity, 27*(9), R123. doi:10.1088/0951-7715/27/9/R123

Pang, S. J. et al. (2010). Tracking the algal origin of the *Ulva* bloom in the Yellow Sea by a combination of molecular, morphological and physiological analyses. *Marine Environmental Research, 69*(4), 207-215. doi:https://doi.org/10.1016/j.marenvres.2009.10.007

Paumier, A. et al. (2018). Impacts of green tides on estuarine fish assemblages. *Estuarine, Coastal and Shelf Science, 213*, 176-184. doi: https://doi.org/10.1016/j.ecss.2018.08.021

Peng, F. et al. (2022). Stochastically Perturbed Parameterizations for the Process-Level Representation of Model Uncertainties in the CMA Global Ensemble Prediction System. *Journal of Meteorological Research, 36*(05), 733-749. doi: 10.1007/s13351-022-2011-8

Qi, L. et al. (2014). Selective ensemble-mean technique for tropical cyclone track forecast by using ensemble prediction systems. *Quarterly Journal of the Royal Meteorological Society, 140*(680), 805-813. doi:https://doi.org/10.1002/qj.2196

Qiao, F. et al. (2009). Banded structure of drifting macroalgae. *Marine Pollution Bulletin, 58*(12), 1792-1795. doi:https://doi.org/10.1016/j.marpolbul.2009.08.006

Qiao, X. S. et al. (2023). Impacts of the stochastically perturbed parameterization on the precipitation ensemble forecasts of the Betts-Miller-Janji<acute accent>c (BMJ) scheme in Eastern China. *Atmospheric Research, 295*. doi:10.1016/j.atmosres.2023.107036

Robinson, C. L. K. et al. (2021). Comparison of spatial distribution models to predict subtidal burying habitat of the forage fish in the Strait of Georgia, British Columbia, Canada. *Aquatic Conservation: Marine and Freshwater Ecosystems, 31*(10), 2855-2869. doi:https://doi.org/10.1002/aqc.3593

Roiha, P. et al. (2010). Ensemble forecasting of harmful algal blooms in the Baltic Sea. *Journal of Marine Systems, 83*(3), 210-220. doi:https://doi.org/10.1016/j.jmarsys.2010.02.015

Sheng, H. et al. (2023). A multi-module with a two-way feedback method for *Ulva* drift-diffusion. *Acta Oceanologica Sinica, 42*(12), 118. doi: 10.1007/s13131-023-2165-y

Wang, S. et al. (2022). Distribution characteristics of green tides and its impact on environment in the Yellow Sea. *Marine Environmental Research, 181*, 105756. doi:https://doi.org/10.1016/j.marenvres.2022.105756

Weber, H. C. (2003). Hurricane Track Prediction Using a Statistical Ensemble of Numerical Models. *Monthly Weather Review, 131*(5), 749-770. doi:https://doi.org/10.1175/1520-0493(2003)131<0749:HTPUAS>2.0.CO;2

Weigel, A. P. et al. (2009). Seasonal Ensemble Forecasts: Are Recalibrated Single Models Better than Multimodels? *Monthly Weather Review, 137*(4), 1460-1479. doi:https://doi.org/10.1175/2008MWR2773.1

Wu, H., Levinson, D. (2021). The ensemble approach to forecasting: A review and synthesis. *Transportation Research Part C: Emerging Technologies, 132*, 103357. doi:https://doi.org/10.1016/j.trc.2021.103357

Xing, Q. et al. (2019). Monitoring seaweed aquaculture in the Yellow Sea with multiple sensors for managing the disaster of macroalgal blooms. *Remote Sensing of Environment, 231*, 111279. doi:https://doi.org/10.1016/j.rse.2019.111279

Xing, Q., Hu, C. (2016). Mapping macroalgal blooms in the Yellow Sea and East China Sea using HJ-1 and Landsat data: Application of a virtual baseline reflectance height technique. *Remote Sensing of Environment, 178*, 113-126. doi:https://doi.org/10.1016/j.rse.2016.02.065

Ye, N. H. et al. (2011). 'Green tides' are overwhelming the coastline of our blue planet: taking the world's largest example. *Ecological Research, 26*(3), 477-485. doi:10.1007/s11284-011-0821-8

Yi, L. et al. (2010). Influnce of Environmental Hydro-Meteorological Conditions to Enteromorpha prolifera Blooms in Yellow Sea, 2009. *Periodical of Ocean University of China, 40*(10), 15-23. doi:10.16441/j.cnki.hdxb.2010.10.003

Zhan, Y. et al. (2024). Long-Term Spatiotemporal Characteristics of *Ulva prolifera* Green Tide and Effects of Environmental Drivers on Its Monitoring by Satellites: A Case Study in the Yellow Sea, China, from 2008 to 2023. *Journal of Marine Science and Engineering, 12*(4), 630. doi: https://www.mdpi.com/2077-1312/12/4/630

Zhang, X., Yu, H. (2017). A Probabilistic Tropical Cyclone Track Forecast Scheme Based on the Selective Consensus of Ensemble Prediction Systems. *Weather and Forecasting, 32*(6), 2143-2157. doi:https://doi.org/10.1175/WAF-D-17-0071.1

Zhao, C. et al. (2018). The Modelling of *Ulva Prolifera* Transport in The Yellow Sea and Its Application. *Oceanologia Et Limnologia Sinica, 49*, 1075-1083. doi: http://dx.doi.org/10.11693/hyhz20180400089

Zhao, J. et al. (2018). The Yellow Sea green tide: A risk of macroalgae invasion. *Harmful Algae, 77*, 11-17. doi:10.1016/j.hal.2018.05.007

Zhou, F. et al. (2021). The Lagrangian-based Floating Macroalgal Growth and Drift Model (FMGDM v1.0): application to the Yellow Sea green tide. *Geosci. Model Dev., 14*(10), 6049-6070. doi:10.5194/gmd-14-6049-2021